STABILITY STUDY OF LAMINAR FLAME USING PROPER ORTHOGONAL DECOMPOSITION AND DYNAMIC MODE DECOMPOSITION

Souvick Chatterjee[1], Achintya Mukhopadhyay*[2], Swarnendu Sen[1]

[1] Department of Mechanical Engineering, Jadavpur University
Kolkata 700 032, India
[2] Department of Mechanical Engineering, IIT Madras
Chennai 600 036, India
* Corresponding author: achintya@iitm.ac.in

Flame dynamics and flickering is a complex problem involving different non linearities. Such a problem has been addressed in this work using two linear orthogonal decomposition techniques for flames in a candle and a burner. The techniques, named as Proper Orthogonal Decomposition (POD) and Dynamic Mode Decomposition (DMD) have been described and used on high speed images. While POD provided measures of the energy content in different modes, through DMD the temporal frequency and growth rates were obtained. An interesting reconstruction technique using POD also allowed interpolation of the contour of the flames in between two high speed snapshots. This is very useful since it helped overcoming the constraint of speed of the camera. A study of interrelation between the two techniques by projecting a DMD mode onto the POD spectrum also provided interesting correlation between POD and DMD modes. This enabled identification of energy content in a specific frequency.

1 Introduction

Flame dynamics is an important topic of study not only because of its immense applications but also owing to the complexities involved. The non-linear and chaotic behavior of the flame arouses substantial interest in the system for many researchers. The dynamics of the flame is a result of powerful coupling between turbulence, combustion and acoustics which lead to combustion instabilities. Different flame dynamics studies exist in the literature which addresses the difficulties associated with this study. Hoinghaus et. al [1] provided an excellent review about different experimental diagnostics tool that have been in use over the years. Using light, i.e. electromagnetic radiation, studies on flame dynamics have been presented in several studies [2–4]. In this work, images are captured using a high speed camera which are post processed in a unique way.
Different established experimental investigations of the flame dynamics include usage of Particle Image Velocimetry (PIV) to capture the flow field in a combustor [5], usage of OH and CH imaging for analysis of heat release fluctuations in swirling flame [6] and to study flame response to acoustic perturbation [7]. Experimental studies on diffusion flames have been limited mainly to study of soot and temperature profiles in a stable laminar flame [8, 9]. Another interesting phenomenon in this context is flame flickering which is well known and has been extensively studied [10]. This buoyancy driven instability is yet to be fully understood and the current study of such flames from both a burner and candle provide interesting information regarding the non linear dynamics associated with it. These kind of flame investigations and study of their characteristics are also helpful for studies on fire investigation. This has

been elaborately explained by Hamins et. al [11] through elaborate study of structure of candle frames using both experimental and modeling techniques. Flickering in candle flames has also been studied by placing the candle in hollow cylindrical tubes by Ghosh et . al [12]. The latter work has characterized the candle flame using a camera as well as a Photo-Multiplier Tube (PMT) and ananlyzed the periodicity in the signal using correlation dimension. However, all these techniques of analyzing the flame dynamics fail to capture the interaction of the flame with large scale coherent structures as many information contained in the snapshots is lost owing to the post processing techniques applied. Few techniques have the ability to project the data and extract the coherent components which includes conditional averaging, wavelet analysis [13] and Orthogonal Mode Decomposition techniques [14]. Presently, we focus on two of these recent Decomposition Techniques namely Proper Orthogonal Decomposition and Dynamic Mode Decomposition to study and understand the complex non-linearities associated with flame dynamics.

The Proper Orthogonal Decomposition (POD) technique emerged as a powerful decomposition tool to analyze the energetic modes in a flow [15]. The method is capable of extracting flow information from the snapshots and hence is applicable to experimental data [16]. The method determines the most energetic structure by diagonalizing the spatial correlation matrix computed from the snapshots. The mode containing the highest amount of energy in the norm is considered as the first mode. They are arranged in decreasing order of mode. POD is currently extensively used in turbulent and unsteady flows [15, 17], combustion related studies [18, 19], analysis of blowoff in flames [20] and also in atomization and sprays [21]. A recent extension of this algorithm is the use of Extended POD that has been used by Duwig and Iudiciani [22] on PIV and OH-PLIF images to reveal interesting flow features about unsteady flames. Vaughan and Renfro [23] used POD to identify phase-resolved flame fronts of premixed flames. Using this technique on relatively simpler chemiluminescence imaging as compared to OH-PLIF, they studied thermo-acoustic coupling in Rijke tube. Another interesting advantage of POD is reconstructing the flow field and obtaining data at off-design parameters as has been shown in numerical results by Ding et. al [24]. Similar method has also been incorporated in this study for experimental high speed images to obtain information at time intervals in between two snapshots. But, in POD, the time component is generally not resolved and hence limited interpretation in the form of energy content is only available.

The other decomposition technique, known as Dynamic Mode Decomposition (DMD) is a relatively new concept proposed and used extensively by Schmid [25, 26]. This technique is based on Koopman modes [27] and extracts data from snapshots associating a frequency to each mode. For combustion and flame dynamics, frequency plays an important role and hence such study is crucial. Apart from the temporal frequency, the growth rate associated with a specific frequency can also be obtained from such an analysis. In combustion and flame related studies, this analysis is pretty unique and has been adopted in this work. One interesting post processing is a combination of POD and DMD that have been highlighted by Muld et. al [28] in numerical simulation of a high speed train. Such a concept has been also proposed by Schmid [25] who mentioned about combining the two modes such that energy content in a particular mode of temporal frequency can be obtained. Other works combining both of these decomposition techniques include those of Semeraro et. al [29], Chatterjee et. al [30] and Singh et. al [31].

In this work, high speed images are captured of a laminar flame of both a candle and a non premixed burner. The images are post processed using both POD and DMD techniques. The nonlinear phenomenon driving the flame dynamics has been analyzed through different modes of both the techniques. Finally, a correlation between POD and DMD has been shown which led to identification of the growth rate and temporal frequency of a POD mode with particular energy content.

2 Decomposition Methods

The starting point of both the decomposition techniques is a temporal sequence of N data fields arranged in a matrix U:

$$U = [u_1, u_2, ..., u_N] \tag{1}$$

Each flow field u_j contains the intensity of a frame at jth time instant, the size of the vector being the net pixel size of the image (row size x column size).

2.1 Proper Orthogonal Decomposition

POD proceeds by decomposing the field into a set of basis functions and mode coefficients, such that:

$$u(x,t) = \sum_{i=1}^{N_m} a_i(t)\sigma_i(x) \tag{2}$$

where σ_i(x)are the spatial basis functions, $a_i(t)$ the mode coefficients and N_m is the finite number of modes. A temporal correlation matrix, C is calculated such that

$$C = U^T U \tag{3}$$

which expresses the difference between any two snapshots. The solution of the linear eigenvalue problem

$$C\phi_j = \lambda_j \phi_j \tag{4}$$

allows the construction of the mode ϕ_j. The symmetry of the correlation matrix demands the eigenvalues λ_j to be real and the energy content of the coherent flow structure are represented by the eigenvectors ϕ_j. The orthogonality of the eigenvectors statistically decorrelates two POD modes.
Another interesting analysis that follow this POD analysis is reconstruction of the snapshots by combination of the eigenvectors, sorted in descending order of their eigenvalues as suggested by Ding et. al [24]. The reconstruction is given by the equation:

$$u(x,t_n) = \phi_{mean} + \sum_{k=1}^{N_m} \alpha_k(t_n)\phi^k(x) \tag{5}$$

where ϕ_{mean} is the mean mode and emperical constants $\alpha_k(t_n)$ are found by projecting flow fields onto eigenfunctions such that:

$$\alpha_k(t_n) = < u(x,t_n), \phi^k(x) > \tag{6}$$

where <x,y> denotes inner product of x and y. The time interval between two snapshots is decided by the sampling frequency of the camera. The Prosilica high speed camera used in this work enabled capturing of the images at 340 fps and 360 fps for the candle and burner flame respectively. Hence, this reconstruction method from POD provided information about the flame dynamics at the intermediate time intervals. Also, certain energy coefficients have been defined in the literature [24]. These are named as:

- Participating Energy Coefficient, ζ_n, representing the fractional energy in n^{th} mode expressed as:

$$\zeta_n = \frac{\lambda_n}{\sum_{n=1}^{N} \lambda_n} \tag{7}$$

- Cumulative Energy Coefficient, η_n, providing a measure of the increment in total energy content with increasing mode number, is given by:

$$\eta_n = \frac{\sum_{n=1}^{N_m} \lambda_n}{\sum_{n=1}^{N} \lambda_n} \tag{8}$$

2.2 Dynamic Mode Decomposition

DMD considers the Koopman operator (A) of the classical Arnoldi idea to express the mapping underlying the snapshot basis. Koopman operator is defined as a linear operator such that

$$u_{j+1} = Au_j \tag{9}$$

Mathematically following the idea underlying Krylov techniques [32], this translates into

$$U_2^N = U_1^{N-1} S \tag{10}$$

where S is a companion matrix that approximates the last snapshot N by a linear combination of the previous N-1 snapshots. It is well-known that eigenvalues of S, also known as the Ritz values will approximate some of the eigenvalues of the full system matrix A. In this formulation, the temporal information is given by the real and imaginary part of the eigenvalues of S, with the real part as the growth/decay rate and the imaginary part as the frequency of the associated dynamic mode. The full algorithm for analysis of the dynamic mode spectrum and the associated modes is presented very well in [26].
The time evolution of the POD modes is described by arbitrary functions $a_i(t)$, whereas in DMD they are measured from the complex eigenvalues of the Koopman operator. Hence, in DMD, each mode oscillates at a single frequency providing orthogonality in time. However the POD modes are orthogonal in space and provides measures of the energy content. Therefore, if a specific DMD mode is projected onto the POD spectrum, energy content values of that particular mode can be known. Thus complete information of a particular mode in the form of temporal frequency, growth rate and energy content are known from this combination of the two decomposition techniques. Hence, a comprehensive knowledge is obtained about the complex non linear processes associated with the flame dynamics using these two linear decomposition techniques.

3 Results

In this work, two different flames have been analyzed using the decomposition techniques discussed earlier. For both the systems, high speed images were captured using a Prosilica High Speed Camera at 614 frames per second. These images are processed to understand the underlying non linear complexities present in the flames. In this section, first the POD modes along with the associated fractional energy content are presented. This is followed by utilization of an unique reconstruction technique using POD to obtain the contour plot of the images at time intervals that fall in between two high speed snapshots. This technique takes care of the constraint of absence of a higher speed camera. Subsequently, the DMD modes corresponding to temporal frequencies present in the particular flame is obtained. Finally, the correlation between the two techniques is established by projecting a specific DMD mode onto the POD spectrum. This comprehensive analysis also allowed a complete understanding of a particular mode of instability with knowledge of its temporal frequency, growth rate and energy content.

3.1 Candle Flame

3.1.1 POD Modes

A typical candle flame captured is shown in Fig. 1. POD is done a temporal sequence of 1000 such images captured at a sampling frequency of 614 fps.

The different modes corresponding to the eigenvalues are shown in Fig. 2. The first figure in top left corner represents the mean flow with largest energy content. As can be seen in Fig. 2, contour plots of the higher modes show interesting spatial structures formed in the region of interest. These structures are important for studying the flickering of the flame which is owing to an inherent instability in the system. The mean flow is followed by a mode with a pair of counter rotating vortices such that the number of vortices increases with mode number.

The measures of energy in the form of net energy content, fractional energy content and cumulative energy content in a mode have been tabulated in Table 1. As can be seen, the mean or non-fluctuating

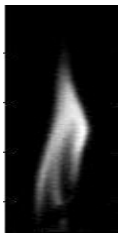

Figure 1: A Typical Candle Flame

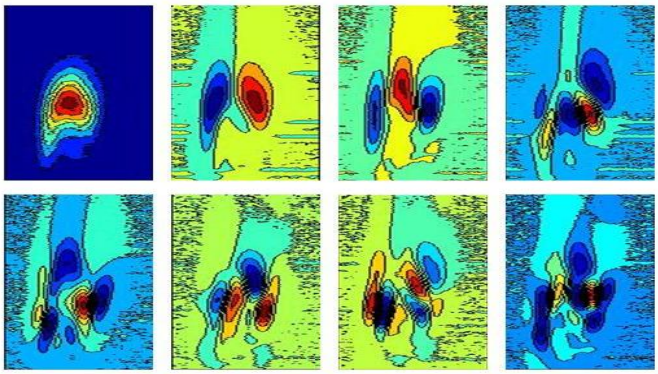

Figure 2: Different modes in *(clockwise from top left)* Decreasing Order of Energy Content

mode always possess the maximum energy. In this particular case, the change in fractional energy content from 5^{th} to 8^{th} mode is not that significant which is also evident from the contour diagrams of the modes.

Table 1: Different Energy Values as obtained from POD for Mean and Higher Fluctuating Modes

i	1 (mean)	2	3	4	5	6	7	8
λ_i	1.2406e10	1.7037e9	4.5743e8	2.2398e8	1.8615e8	1.4954e8	1.0734e8	7.7266e7
$\zeta_i(\%)$	77.8226	10.6874	2.8695	1.4050	1.1677	0.9381	0.6734	0.4847
$\eta_i(\%)$	77.8226	88.5100	91.3795	92.7845	93.9522	94.8903	95.5637	96.0483

Thus, using POD, underlying details about the flickering phenomenon of a candle flame can be obtained through analysis of higher modes of instability. These energy values are compared with that of a burner later in this paper providing a comparative study between two laminar flames.

3.1.2 Reconstruction using POD

This is an unique advantage of the POD technique as is shown for numerical studies by Ding et. al [24]. Using Eq. 5, contour images at any desired time within the specified interval can be obtained. Thus the limitation of the speed of the camera can be overcome. Capturing the candle flame flickering at 614 fps, frames at an interval of 1.63 ms have been captured. After plotting the empirical coefficient, α obtained through Eq. 6 at design parameters, i.e. at time intervals where the camera snapshot is present, a cubic spline has been fitted to interpolate the empirical coefficients at off-design parameters. This, in turn, leads to accurate prediction of the contour of flames at the off design parameters as can be seen in Fig. 3. For reconstructing the POD images in Fig. 3, only odd images of the high speed sequence were considered. If t_0 denotes the time for initial snapshot, based on the sampling frequency, the four

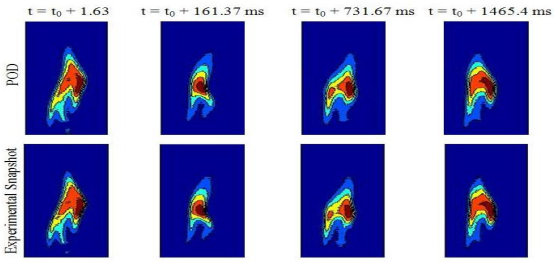

Figure 3: Validation of Flame Contour Images at Off-Design Parameters

time frames in Fig. 3 denote the 2^{nd}, 100^{th}, 450^{th} and 900^{th} image. Hence, the even numbered images were reconstructed using POD reading only the odd numbered high speed snapshot. Thus, the accurate validation at the off-design parameters, allow reconstructing the contour of the flickering flame at time intervals smaller than the frequency of the camera.

3.1.3 DMD Modes

Dynamic Mode Decomposition (DMD) is comparatively a computationally expensive technique. The eigenvectors computed in this technique are sorted in ascending order of the temporal frequencies, i.e. the imaginary part of the eigenvalues. Hence, the first eigenvalue of this sorted order, will show a zero temporal frequency denoting the mean flow. The first modes of the two decomposition techniques, thus represent the non-fluctuating part and hence are similar.

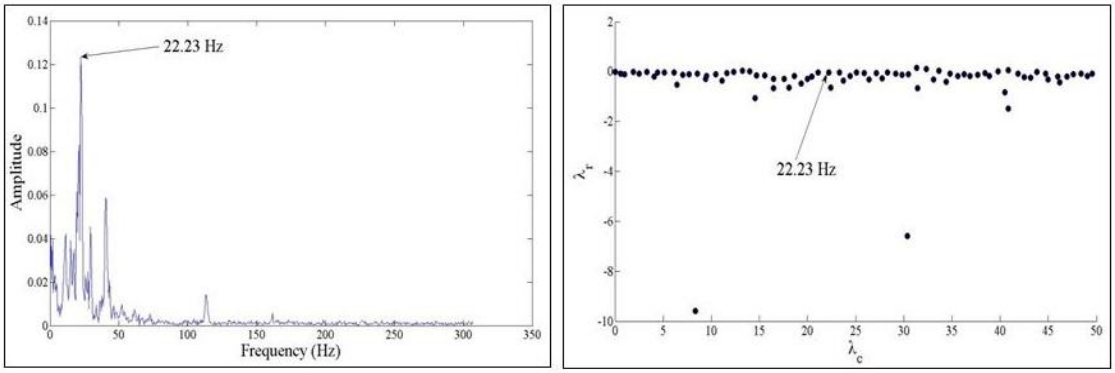

Figure 4: *(left)* FFT based on Mean Intensity and *(right)* DMD Spectrum With Positive Frequencies

First, the flickering frequency of the candle flame is estimated by a Fast Fourier Transform (FFT) of the mean intensity of the temporally varying frames. Then, from the entire DMD spectrum, the zone with temporal frequencies in proximity to major frequencies obtained from the FFT is identified. The temporal frequencies correspond to imaginary part of the eigenvalues, i.e. λ_c. The frequencies occur in pair and only the positive values are shown in the spectrum in Fig. 4. The y-axis in the DMD spectrum denote the real part of the eigenvalues, λ_r, the absolute value of which is a measure of the growth rate of the instability associated with the flame flickering. The DMD eigenvalues are sorted in ascending order of their magnitude, such that the mean mode with 0 frequency denotes the non-fluctuating mode. In the sorted DMD spectrum, the mode with eigenvalue similar to the FFT frequency is identified. The frequency of 22.23 Hz with highest amplitude turned out to be DMD Mode 70, whereas certain frequencies like 21.09 Hz and 40.84 Hz with lower amplitudes have also been found which corresponded to DMD Mode 68 and 132 respectively. The DMD contours of all these modes have been shown in Fig. 5. Also, the growth rate of these DMD modes can be obtained from the spectrum since the real part of the eigenvalues denote the growth rate. It was found that the frequencies of 21.09 Hz or 22.23 Hz possess a growth

rate of 0.0328 whereas the higher frequency of 40.84 Hz had a growth rate of 0.0576. Thus, knowing, the frequency of the problem, the corresponding dynamic modes and growth rate have been identified using this decomposition technique. The contours of the dynamic modes showed interesting spatial coherent structures formed in the spatial domain of the flickering flame which are crucial for detailed understanding of the complex problem.

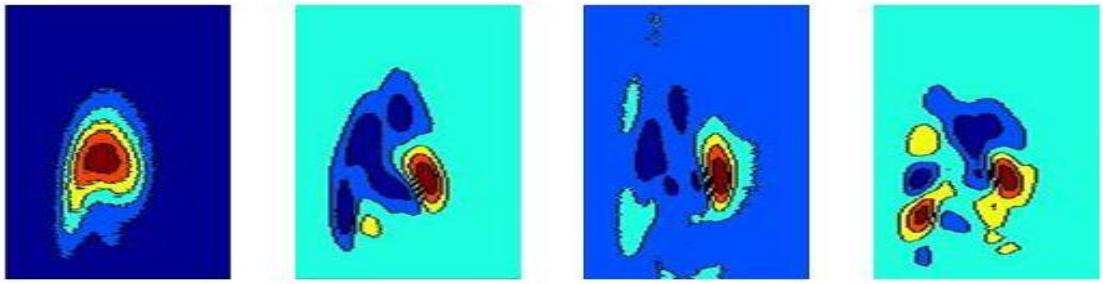

Figure 5: *(from left)* Mean Mode; DMD Mode 68; DMD Mode 70; DMD Mode 132

3.2 Burner Flame

The ability to control the fuel flow rate in the burner allowed analysis of two different flames: a steady and a flickering flame. Thus, effect of this flame nature on the energy, frequency and growth rate values has been shown.

3.2.1 POD Modes

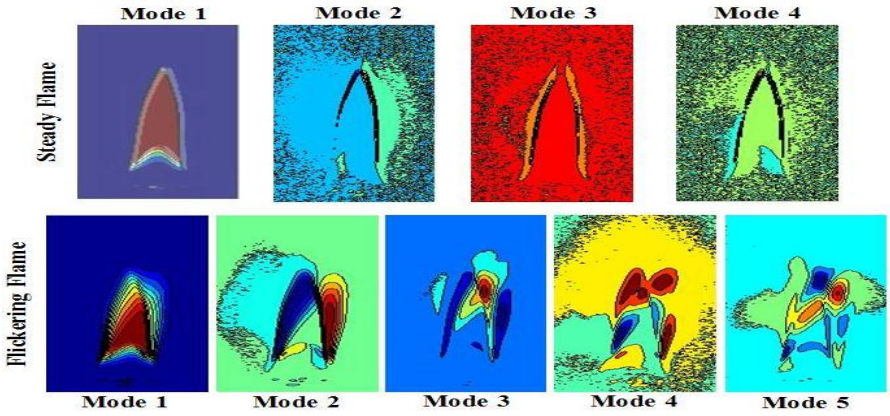

Figure 6: Different POD modes for a Steady and a Flickering Flame of a Burner

A comparative study between a steady and a flickering flame can be made from the higher mode contour diagrams of the flame as is shown in Fig. 6.

For a steady flame, the higher modes hardly show any coherent structures and Mode 4 clearly depicts noise in the image. The edge of the flame from an actual image is superimposed on the mean contour of this flame which can be seen in white colour. However, for a flickering flame, interesting spatial structures can be obtained from the higher modes as is shown in Fig. 6. This phenomenon can also be seen from Fig. 7 where the fractional energy content in each mode is plotted for both a steady and a flickering flame. The higher modes in a steady flame clearly show a decreased energy content as compared to that of a flickering flame which leads to the presence of higher noise in the steady configuration. Hence,

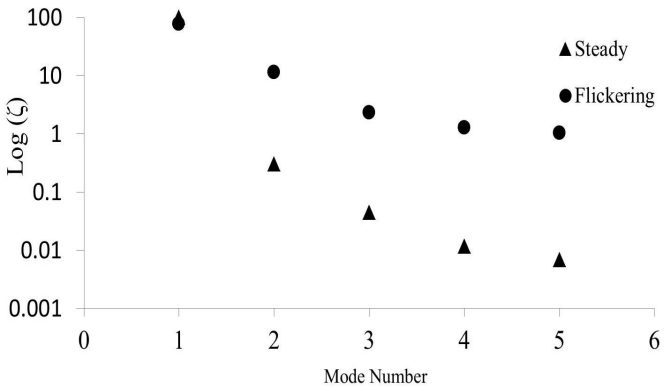

Figure 7: Variation of Participating Energy Coefficients, ζ with Increasing Modes

in a steady flame, the higher modes are insignificant and fail to convey any extra information. However, for a turbulent highly flickering flame, the higher modes containing significant energy is useful to understand the complexity of the problem.

3.2.2 DMD Modes

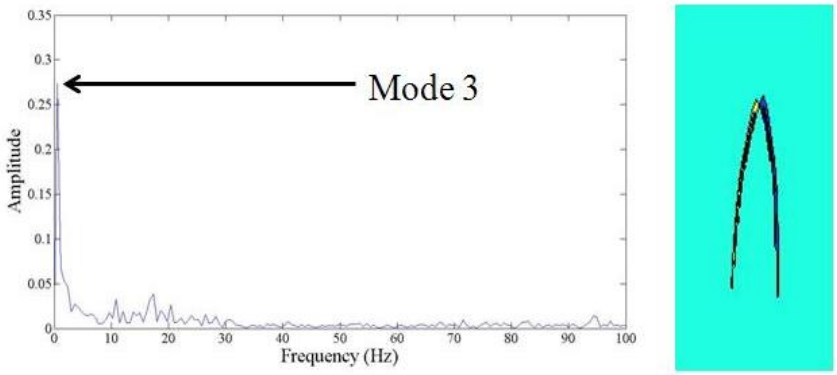

Figure 8: *(left)* FFT of A Steady Burner Flame and *(right)* Corresponding Contour of the Dominant Frequency

Figure 8 clearly shows the presence of a single dominant frequency in the FFT of the mean intensity of the steady flame. The is owing to the highly laminar nature of the flame. This frequency turned out to be the 3rd mode in the sorted eigenvalue order and the corresponding contour of the flame of this mode is also shown in Fig. 8. The frequency and growth rate, as obtained from the DMD analysis, are 0.5497 Hz and 0.6212 respectively. The high steadiness of this flame eliminates the need for any other modes of this analysis. Essential, those modes are expected to produce significant noise.

On the other hand, the FFT of the turbulent flickering flame shows the presence of different frequencies as is shown in Fig. 9. The frequencies with significant amplitude dominate the flame dynamics and hence are identified in the DMD spectrum. From the sorted eigenvalue list, the mode numbers corresponding to some of these dominant frequencies have been found and contours of those modes are analyzed. As expected the mean mode, representing the non fluctuating zero frequency mode, remains similar in both the decomposition techniques. Figure 9 shows most of the dominant frequencies in the 0-50 Hz regime. Four such frequencies evenly distributed in the spectrum showing high amplitude have been identified as 1.38 Hz, 13.64 Hz, 27.62 Hz and 43.74 Hz. The contours of these four frequencies

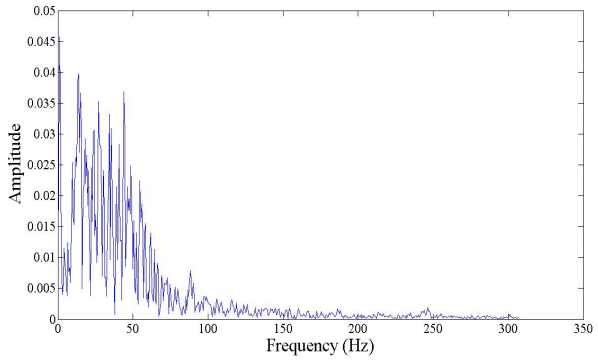

Figure 9: FFT of Mean Intensity of a Highly Flickering Flame

along with that of the mean are shown in Fig. 10.

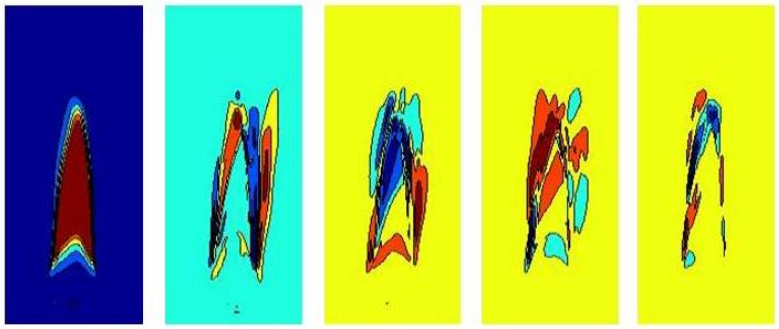

Figure 10: *(From Left)* Mean Mode; Mode 6; Mode 44; Mode 88; Mode 140

Interesting spatial coherent structures showing the instability associated with flickering of the flame can be seen from the contours of the higher modes. In case of a steady flame a particular frequency heavily dominates the process leading to a single important higher mode. But, in contrast, for a turbulent flickering flame, the energy gets dissipated among many frequencies and hence those frequencies convey important information through the eigen modes. Also, similar to above cases, the growth rates of these modes are also known from real part of the eigenvalues. As expected, the mean mode shows least growth rate whereas modes 6, 44, 88 and 140 have growth rates of 0.1543, 0.1731, 0.1338 and 0.379 respectively.

3.2.3 Relating POD and DMD

The two modes show interesting results about the complicated flame flickering problem. A comparison and correlation between the two methods is important for a two fold purpose:

- Understanding the advantages and disadvantages of two important and useful Decomposition Methods
- Correlating the two methods such that a comprehensive analysis can be performed on this complex instability problem.

In this section, it is shown that if a specific DMD mode with a particular temporal frequency and growth rate is projected onto the POD spectrum, high correlation is obtained at one or more POD modes. Again, since each POD mode represents a particular energy content, the amount of fractional

energy in the specific frequency is obtained. If $r_{DMD_i,POD}$ denotes the correlation coefficient of i^{th} DMD mode with the POD spectrum,

$$r_{DMD_i,POD} = \sum_{j=1}^{n} < \phi_{DMD_i}, \phi_{POD\,j} > \tag{11}$$

The mean non-fluctuating modes being similar in the two decomposition techniques, are expected to have exact correlation. Hence, an exact correlation is obtained between the first modes

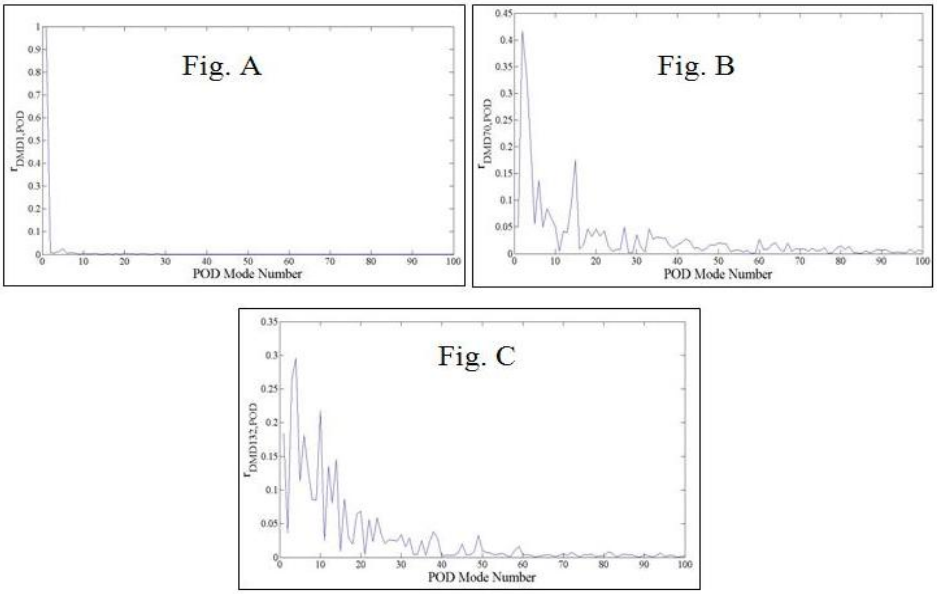

Figure 11: Projection of DMD Mode 1(Fig. A), 70 (Fig. B) and 132 (Fig. C) onto POD spectrum

Figure 11 shows DMD Mode 70 to have best correlation with POD Mode 2 whereas DMD Mode 132 is correlated with POD Mode 4. Hence, the temporal frequencies of DMD are also related to energies obtained from POD. So, DMD Mode 70 known to have a temporal frequency of 22.23 Hz is expected to have a fractional energy of 10.6874% as this mode is found to be mostly correlated to 2^{nd} POD mode. However, the higher DMD Mode 132 is found to be loosely correlated to multiple POD modes as can be seen from the many short peaks in Fig. 11 C.

Similar analysis of the burner flame also showed interesting features about this non linear problem. As can be seen from Fig. 12, DMD Mode 6 correlates with POD Modes 3 and 7 and FFTs of both these POD modes show the frequency shown in Fig. C. This corresponds to a highly flickering flame, FFT of mean intensity of which is shown in Fig. 9. But, DMD Mode 6 has a low frequency of 1.38 Hz as is mentioned in the earlier section. The FFT of the POD Modes which are found to be correlated with DMD Mode 6 also show a low frequency of 1.202 Hz which validates the mapping between the two decompositions. But a higher DMD Mode like Mode 140 having a temporal frequency of 43.74 Hz has also substantial correlations with higher modes like POD Mode 11 with a lower fractional energy content. The higher frequencies of the flame found in Fig. 9 show up in the FFT of this higher POD Mode 11. Thus, for such a turbulent flickering flame, an interrelation between POD and DMD provide details of the growth rate and energy content in all the relevant frequencies of the phenomenon.

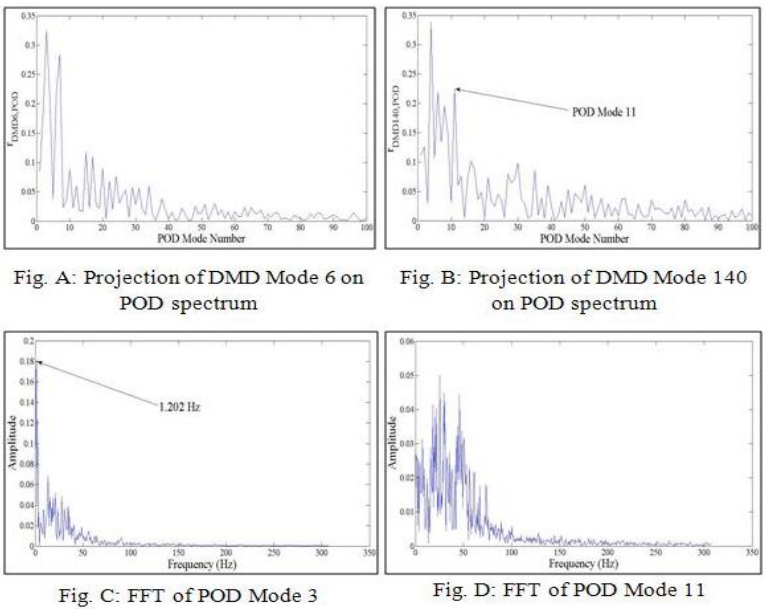

Fig. A: Projection of DMD Mode 6 on POD spectrum

Fig. B: Projection of DMD Mode 140 on POD spectrum

Fig. C: FFT of POD Mode 3

Fig. D: FFT of POD Mode 11

Figure 12: Projection of DMD Mode 6(Fig. A) and 140 (Fig. B) onto POD spectrum and FFTs of corresponding correlated POD Modes (Fig. C; Fig. D)

4 Conclusions

The complex non linear problem of flickering in a flame is studied in this work in a unique way using two linear decomposition techniques in the form of Proper Orthogonal Decomposition and Dynamic Mode Decomposition. Both these algorithms use the intensity of high speed images obtained from a candle and a burner flame as inputs and provide the temporal frequencies, growth rates and energy content in different modes. Also, contours of different modes provide interesting information about the presence of coherent structures in the phenomenon.

The POD technique provides measure of fractional energy content in different modes. The mean non fluctuating mode contains maximum energy and it decreases with increasing mode. Presence of coherent structures in the form of counter rotating vortices can be seen from the contours. Also, with increase in mode number, number of such vortices increases. Apart from this, an interesting advantage of POD as shown, is interpolating the contours of flame at off-design parameters, *i.e.* at time intervals where experimental snapshot is absent owing to limitation in the form of speed of the camera.

The other technique, Dynamic Mode Decomposition, is important for understanding temporal details about the problem. The frequencies pertinent in the problem have been identified in the DMD eigenvalue spectrum where the DMD complex eigenvalues are plotted in an imaginary plane. The growth rates of the DMD modes with relevant temporal frequencies are given by the real part of the eigenvalues. Another interesting inclusion in this work is projection of a specific DMD mode onto the POD spectrum. This highlighted the correlation between the two techniques. As expected, the mean of the two methods are very strongly correlated as they represent the non-fluctuation part. This correlation provided measure of energy content in a mode with a particular specific frequency. Specially for turbulent, highly flickering complex flames with different frequencies, such a study allowed separation of the different frequencies and finding out the growth rate and energy contents in them.

References

[1] Katharina Kohse-Hoinghaus, Robert S. Barlow, Marcus Alden, and Jurgen Wolfrum. Combustion at the focus: laser diagnostics and control. *Proceedings of the Combustion Institute*, 30(1):89–123,

2005.

[2] Erhard W. Rothe, Yong-Wei Gu, and Gene P. Reck. Laser-induced predissociative fluorescence: dynamics and polarization and the effect of lower-state rotational energy transfer on quantitative diagnostics. *Appl. Opt.*, 35(6):934–947, 1996.

[3] J. W. Daily. Laser induced fluorescence spectroscopy in flames. *Progress in Energy and Combustion Science*, 23(2):133–199, 1997.

[4] Normand M. Laurendeau. Temperature measurements by light-scattering methods. *Progress in Energy and Combustion Science*, 14(2):147–170, 1988.

[5] Sebastian Pfadler, Frank Beyrau, and Alfred Leipertz. Flame front detection and characterization usingconditioned particle image velocimetry (cpiv). *Opt. Express*, 15(23):15444–15456, 2007.

[6] Balachandran R. Frank J. H. Mastorakos E. Ayoola, B. O. and C. F. Kaminski. Spatially resolved heat release rate measurements in turbulent premixed flames. *Combustion and Flame*, 144(1-2):1–16, 2006.

[7] R. Balachandran, B. O. Ayoola, C. F. Kaminski, A. P. Dowling, and E. Mastorakos. Experimental investigation of the nonlinear response of turbulent premixed flames to imposed inlet velocity oscillations. *Combustion and Flame*, 143(1-2):37–55, 2005.

[8] Decio S. Bento, Kevin A. Thomson, and Omer L. Gulder. Soot formation and temperature field structure in laminar propane air diffusion flames at elevated pressures. *Combustion and Flame*, 145(4):765–778, 2006.

[9] Wonnam Lee and Yong Dae Na. Soot study in laminar diffusion flames at elevated pressure using two-color pyrometry and abel inversion. *JSME International Journal Series B*, 43(4):550–555, 2000.

[10] Hamidreza Gohari Darabkhani and Yang Zhang. Methane diffusion flame dynamics at elevated pressures. *Combustion Science and Technology*, 182(3):231–251, 2010.

[11] Anthony Hamins, Matthew Bundy, and Scott E. Dillon. Characterization of candle flames. *Journal of Fire Protection Engineering*, 15(4):265–285, 2005.

[12] Suvojit Ghosh, Sirshendu Mondal, Tanmoy Mondal, Achintya Mukhopadhyay, and Swarnendu Sen. Dynamic characterization of candle flame. *International Journal of Spray and Combustion Dynamics*, 2(3):267–284, 2010.

[13] Katsunori Yoshimatsu, Naoya Okamoto, Kai Schneider, Marie Farge, and Yukio Kaneda. *Wavelet-Based Extraction of Coherent Vortices from High Reynolds Number Homogeneous Isotropic Turbulence*, volume 4 of *IUTAM Bookseries*, chapter 37, pages 243–248. Springer Netherlands, 2008.

[14] TomasW Muld, Gunilla Efraimsson, and DanS Henningson. Mode decomposition on surface-mounted cube. *Flow, Turbulence and Combustion*, 88(3):279–310, 2012.

[15] G Berkooz, P Holmes, and J L Lumley. The proper orthogonal decomposition in the analysis of turbulent flows. *Annual Review of Fluid Mechanics*, 25(1):539–575, 1993.

[16] J. P. Bonnet, D. R. Cole, J. Delville, M. N. Glauser, and L. S. Ukeiley. Stochastic estimation and proper orthogonal decomposition: Complementary techniques for identifying structure. *Experiments in Fluids*, 17(5):307–314, 1994.

[17] S. S. Ravindran. A reduced-order approach for optimal control of fluids using proper orthogonal decomposition. *International Journal for Numerical Methods in Fluids*, 34(5):425–448, 2000.

[18] M. Stohr, R. Sadanandan, and W. Meier. Phase-resolved characterization of vortex-flame interaction in a turbulent swirl flame. *Experiments in Fluids*, 51(4):1153–1167, 2011.

[19] Mark Fogleman, John Lumley, Dietmar Rempfer, and Daniel Haworth. Application of the proper orthogonal decomposition to datasets of internal combustion engine flows. *Journal of Turbulence*, page N23, 2004.

[20] Kristin M. Kopp-Vaughan, Trevor R. Jensen, Baki M. Cetegen, and Michael W. Renfro. Analysis of blowoff dynamics from flames with stratified fueling. *Proceedings of the Combustion Institute*, 34(1):1491–1498, 2013.

[21] Marco Arienti and Marios C. Soteriou. Time-resolved proper orthogonal decomposition of liquid jet dynamics. *Physics of Fluids*, 21(11):112104–15, 2009.

[22] Christophe Duwig and Piero Iudiciani. Extended proper orthogonal decomposition for analysis of unsteady flames. *Flow, Turbulence and Combustion*, 84(1):25–47, 2010.

[23] Kristin Kopp-Vaughan and Michael Renfro. Flame shape and spatially resolved rayleigh criterion using proper orthogonal decomposition. *International Journal of Spray and Combustion Dynamics*, 4(3):255–274, 2012.

[24] Peng Ding, Xue-Hong Wu, Ya-Ling He, and Wen-Quan Tao. A fast and efficient method for predicting fluid flow and heat transfer problems. *J Heat Transfer*, 130(3):032502–032517, 2008.

[25] Peter J. Schmid. Dynamic mode decomposition of numerical and experimental data. *Journal of Fluid Mechanics*, 656:5–28, 2010.

[26] P. J. Schmid. Application of the dynamic mode decomposition to experimental data. *Experiments in Fluids*, 50(4):1123–1130, 2011.

[27] Igor Mezic. Analysis of fluid flows via spectral properties of the koopman operator. *Annual Review of Fluid Mechanics*, 45(1):357–378, 2013.

[28] Tomas W. Muld, Gunilla Efraimsson, and Dan S. Henningson. Flow structures around a high-speed train extracted using proper orthogonal decomposition and dynamic mode decomposition. *Computers & Fluids*, 57(0):87–97, 2012.

[29] Onofrio Semeraro, Gabriele Bellani, and Fredrik Lundell. Analysis of time-resolved piv measurements of a confined turbulent jet using pod and koopman modes. *Experiments in Fluids*, 53(5):1203–1220, 2012.

[30] S. Chatterjee, A. Mukhopadhyay, and S. Sen. Dynamic mode decomposition of liquid jet atomization in a hybrid atomizer. In *National Propulsion Conference-Paper No. 12009*, 2013.

[31] Gaurav. Singh, S. R. Chakravarthy, Biswajit. Banik, and S. Ramgopal. Experimental investigation of primary atomization of liquid jet in subatomic crossflow using proper orthogonal decomposition (pod) and dynamic mode decomposition (dmd). In *National Propulsion Conference-Paper No. 12010.*, 2013.

[32] A. Greenbaum. *Iterative Methods for Solving Linear Systems*. Society for Industrial and Applied Mathematics, 1987.